Green Chemistry

PAPER

View Article Online
View Journal | View Issue

Cite this: *Green Chem.*, 2026, **28**, 3662

Breaking new ground in direct mechanocatalysis: Knoevenagel condensation *via* supported organo-catalysts on zirconia

Maxime Provost,[a] Joao Tanepau,[b,c] Thierry Buffeteau,[d] Marie Gressier,[a] Frédéric Lamaty,[b] Julien Pinaud,*[c] Xavier Bantreil,*[b,e] Marie-Joëlle Menu[a] and Sandrine Duluard*[a]

Mechanocatalysis combines mechanical energy and chemical reactivity to perform solvent-free catalytic transformations. Direct mechanocatalysis involves using reactor-supported catalysts to boost reaction performances while avoiding solvents and energy-consuming post-reaction purification steps. This process aims at increasing the reaction yield and decreasing drastically the E-factor. Herein, we report the first examples of direct mechano-organocatalysis with a piperazine-based organocatalyst, covalently grafted onto amine-functionalized zirconia milling balls. This unprecedented milling system catalyzed Knoevenagel condensations under solvent-free conditions, operating faster (with a thousand-fold less catalyst used than that in traditional methods), achieving full conversion within only3 hours, and remained active after multiple reaction cycles. The turnover frequency (TOF) reached 5700 h^{-1}, far exceeding that of homogeneous analogues (40 h^{-1}), due to the low catalyst loading and efficient energy transfer. Comprehensive surface characterization of the milling balls (XPS and original PM-IRRAS), before and after grafting, and after catalysis, elucidated the structure–activity relationship. This work establishes the first demonstration that a robust organocatalyst can be efficiently used in supported mechanocatalysis, highlighting the promise of surface-engineered zirconia systems for green chemistry.

Received 19th November 2025,
Accepted 16th January 2026

DOI: 10.1039/d5gc06198a

rsc.li/greenchem

Green foundation

1. For the first time, covalently grafted organic catalytic species were shown to resist the demanding conditions of mechanochemistry without performance loss or catalyst release. This highly sustainable and resource-efficient durable organocatalytic system is completely solvent-free, with no solvent required for either the reaction or the purification.
2. This system addresses most of the pillars of green chemistry owing to zero use of solvent (both for the reaction and separation of chemicals) during the catalytic reaction: no waste production, atom economy, safer solvents, catalysis and energy efficiency. The specific green chemistry achievement is a high RME factor (around 90%) with an E-factor of nearly 0 (0.2), much lower than in equivalent solution chemistry or mechanochemical reactions (22 and 17, respectively).
3. The demonstrated concept of direct mechano-organocatalysis with catalysts supported on the milling system could be made greener by increasing the number of available catalytic sites to decrease the reaction time; tuning the nature of the catalyst will open large opportunities in future research.

Introduction

Organic catalytic synthesis without the use of transition metals has significantly transformed modern chemistry. Inspired by biological processes, organocatalysis enables the efficient formation of complex organic molecules while avoiding the use of expensive or toxic metals.[1,2] It stands as a central pillar of catalysis highlighted by the 2021 Nobel Prize in Chemistry awarded to B. List and D. MacMillan for their foundational work on enamine and iminium activation.[3,4] Over time, organocatalysis has expanded to encompass a wide range of strategies, including covalent activation (*e.g.* carbenes,[5] phosphines[6]) and non-covalent interactions such as hydrogen bonding,[7] ion pairing,[8] and phase-transfer catalysis.[9] Its compatibility with mild conditions, a broad range of solvents, and even solvent-free environments makes it a key tool in sustainable chemistry.

[a]*CIRIMAT, Univ Toulouse, Toulouse INP, CNRS, Toulouse, France. E-mail: sandrine.duluard@utoulouse.fr*
[b]*IBMM, Univ Montpellier, CNRS, ENSCM, Montpellier, France. E-mail: xavier.bantreil@umontpellier.fr*
[c]*ICGM, Univ Montpellier, CNRS, ENSCM, Montpellier, France. E-mail: julien.pinaud@umontpellier.fr*
[d]*Université de Bordeaux, ISM, UMR 5255 CNRS, 351 Cours de la Libération, 33405 Talence, France*
[e]*Institut Universitaire de France (IUF), France*

Organocatalysis also integrates well with alternative activation methods such as microwave, ultrasound, and mechanochemical techniques.[10–13]

In this context, mechanochemistry has recently emerged as a powerful technology, enhancing the sustainability, efficiency, and practicality of chemical transformations.[14–16] It enables the activation of solid reagents through mechanical energy, typically *via* a planetary (pbm) or vibratory ball-mill (vbm), facilitating solvent-free transformations and avoiding the use of often toxic and volatile organic solvents.[17] It is particularly well suited for the synthesis of bioactive compounds and pharmaceutical ingredients.[18] In 2006, Bolm's group demonstrated the efficiency of an L-proline-catalyzed aldol reaction under solvent-free ball-milling conditions, paving the way for the merger of organocatalysis and mechanochemistry.[19] Since then, numerous transformations have been developed using this combined approach, employing both covalent and non-covalent activation mechanisms with promising results.[20] In these approaches, the catalyst is added to the reaction media and must be separated afterwards from the desired product. Another concept developed for combining ball-milling and metallic catalysis is "direct mechanocatalysis".[21–24] This concept represents a major advance in sustainable synthesis as it relies directly on the catalytic activity of the milling media, typically the balls or walls of the jar. It was pioneered by Mack's group in 2009, using a copper milling vessel co-catalyst in the Sonogashira cross-coupling reaction, effectively replacing the conventional copper(I) iodide catalyst (Fig. 1).[21] This discovery marked the beginning of what is now known as direct mechanocatalysis, including the use of metallic vials or metal vials coated with Cu,[21,25,26] Au,[27] Ni,[28] and Pd,[23,24] vial-surface charged with metal powders,[29] and metal-oxide milling media such as zirconia balls.[30]

To extend the possibilities of direct mechanocatalysis to organocatalysis, our original approach proposes the anchoring of catalytically active organic moieties onto the mechanochemical balls. Yttria-stabilized zirconia (YSZ) was selected due to its excellent mechanical properties, which minimize surface abrasion during repeated milling cycles, as well as its high chemical resistance to harsh environments, including acids, bases, and organic solvents. YSZ balls serve both as a support to the catalyst and as an energy-transfer medium, since the catalysis is carried out by a molecular organocatalyst covalently immobilized on the surface of the zirconia balls. Piperazine has already been reported as an efficient organocatalyst in the mechanochemical solvent-free Knoevenagel condensation.[31–33] Based on these findings, our approach was to graft a piperazine analogue onto the surface of YSZ milling balls and to evaluate their performance as catalyst supports for the Knoevenagel condensation under direct mechanocatalysis conditions. Different approaches enabled YSZ to be efficiently functionalized in order to obtain reactive balls that could catalyze the Knoevenagel condensation with excellent conversion and recyclability.

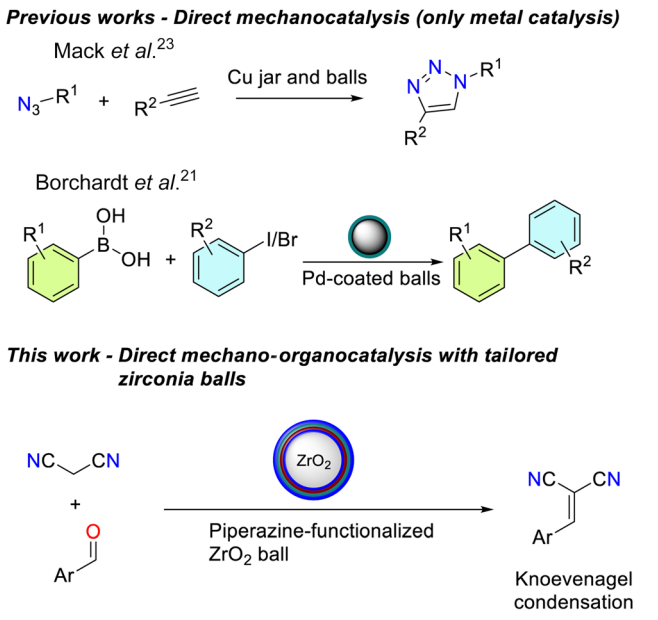

Fig. 1 Concepts for direct mechanocatalysis with metals *vs.* direct mechano-organocatalysis with tailored zirconia balls.

Results and discussion

Functionalization of the YSZ balls

The functionalization strategy involved grafting amine groups that serve as anchoring sites for various catalytically active species. Before functionalization, a surface activation step was performed by immersion of the YSZ balls in a Piranha solution (sulfuric acid and hydrogen peroxide), effectively removing organic contaminants, exposing pre-existing hydroxyl groups, and generating additional surface hydroxyls. Following activation, amine groups were introduced using a surface functionalization agent. Whereas organosilanes are commonly employed for this purpose, reports in the literature indicate that phosphonic acids exhibit greater affinity for metal oxide surfaces such as zirconia.[34] Accordingly, 3-aminopropylphosphonic acid hydrochloride (APPA)[35] was used to covalently anchor amine groups *via* stable Zr–O–P linkages (Fig. 2, **ZrO_2-APPA**). To increase the surface density of amine groups, a second, multistep strategy was developed, involving (i) initial grafting of APPA, (ii) reaction of poly(methylvinyl ether-*alt*-maleic anhydride) (ANHY) with the surface amines to form amide bonds (Fig. 2, **ZrO_2-ANHY**), and (iii) subsequent reaction of the remaining surface anhydride groups with the primary amines of a fourth generation PAMAM dendrimer,[36] which contains 64 terminal primary amines per molecule (Fig. 2, **ZrO_2-PAMAM**).

The amines of the **ZrO_2-APPA** and **ZrO_2-PAMAM** balls were then reacted with bromoethyl-*N*-Boc-piperazine in the presence of KO^{t}Bu, and then treated in acidic and basic media to cleave the Boc protecting group and recover free amines, which are required for further use in organocataly-

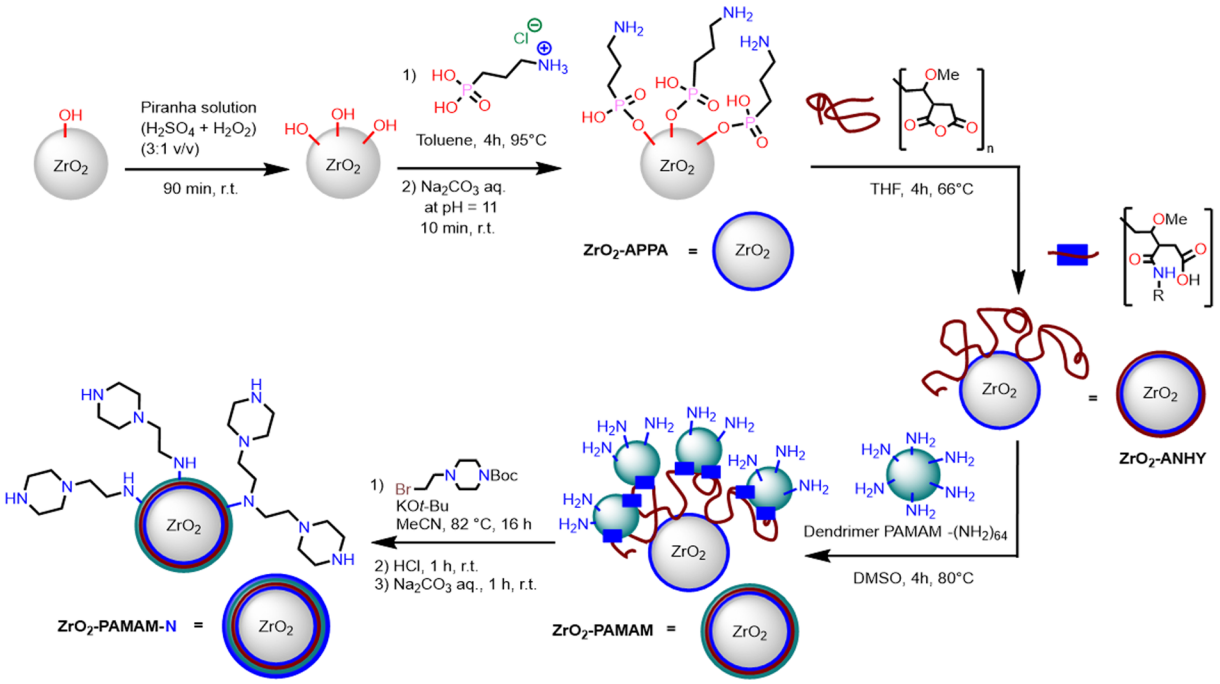

Fig. 2 Strategies for amine functionalization of zirconia milling-ball surfaces.

sis (**ZrO_2-APPA-N** and **ZrO_2-PAMAM-N**). To ensure that our strategy of functionalization would be efficient on milling balls, the same approach was performed on zirconia plates of the same composition as the balls used in mechanochemistry, and which would be easier to analyze and characterize. Polarization-modulation infrared reflection-absorption spectroscopy (PM-IRRAS) and X-ray photoelectron spectroscopy (XPS) experiments were carried out. For the first time, PM-IRRAS was used to characterize organic layers grafted onto YSZ substrates with spectra as presented in Fig. 3. The deconvolution of XPS spectra in the O 1s, C 1s, and Zr 3d regions are reported in Fig. 4, revealing the bonding nature in the synthesized species.

To reveal the very small contribution of the grafted organic layers, it was necessary to subtract the PM-IRRAS spectrum of the non-functionalized zirconia substrate from the PM-IRRAS spectrum of functionalized zirconia substrates (see the supplementary information for details). The successful grafting of APPA on ZrO_2 is evidenced by the presence of several bands on the PM-IRRAS spectrum of **ZrO_2-APPA** (Fig. 3, dark blue curve). The symmetric (ν_sO–P–O) and asymmetric (ν_aO–P–O) stretching vibrations of O–P–O groups are observed at 995 and 1090 cm^{-1}, respectively. The presence of the band at 1250 cm^{-1} is related to the stretching vibration of the P═O groups and reveals the bidentate binding of the phosphonate groups.[37–39] Finally, a broad band is detected around 1500 cm^{-1}, assigned to the symmetric bending vibration of NH_3^+ groups ($\delta_s NH_3^+$).[40] The grafting of APPA on ZrO_2 is also evidenced in XPS spectra within the O 1s region by the presence of the peak at 531.0 eV corresponding to P–OH and P–O–Zr bonds and the component around 532.8 eV related to P═O groups or adsorbed water (H_2O), and in the Zr 3d region by the presence of the two components at 182.7 and 185.1 eV attributed to Zr–O–P interactions.[41,42]

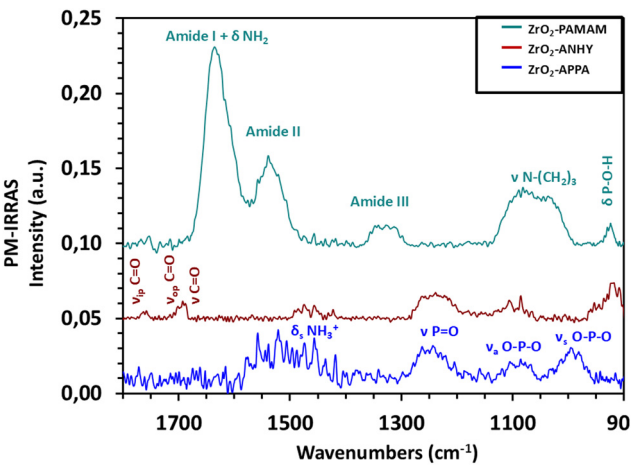

Fig. 3 PM-IRRAS spectra of zirconia plates functionalized with APPA (in dark blue); functionalized with APPA followed by ANHY (in dark red); and functionalized with APPA, then ANHY, and finally 4th generation PAMAM dendrimer (in turquoise).

Upon reaction with the polyanhydride (**ZrO_2-ANHY**), new bands at 1760, 1700 and 1690 cm^{-1} appear, while the decrease of the amine band suggests the grafting of ANHY by amide bond formation. The two bands at 1760 and 1700 cm^{-1} can be assigned to unreacted anhydride carbonyls (in-phase and out-of-phase stretching vibrations of the two C═O groups, respect-

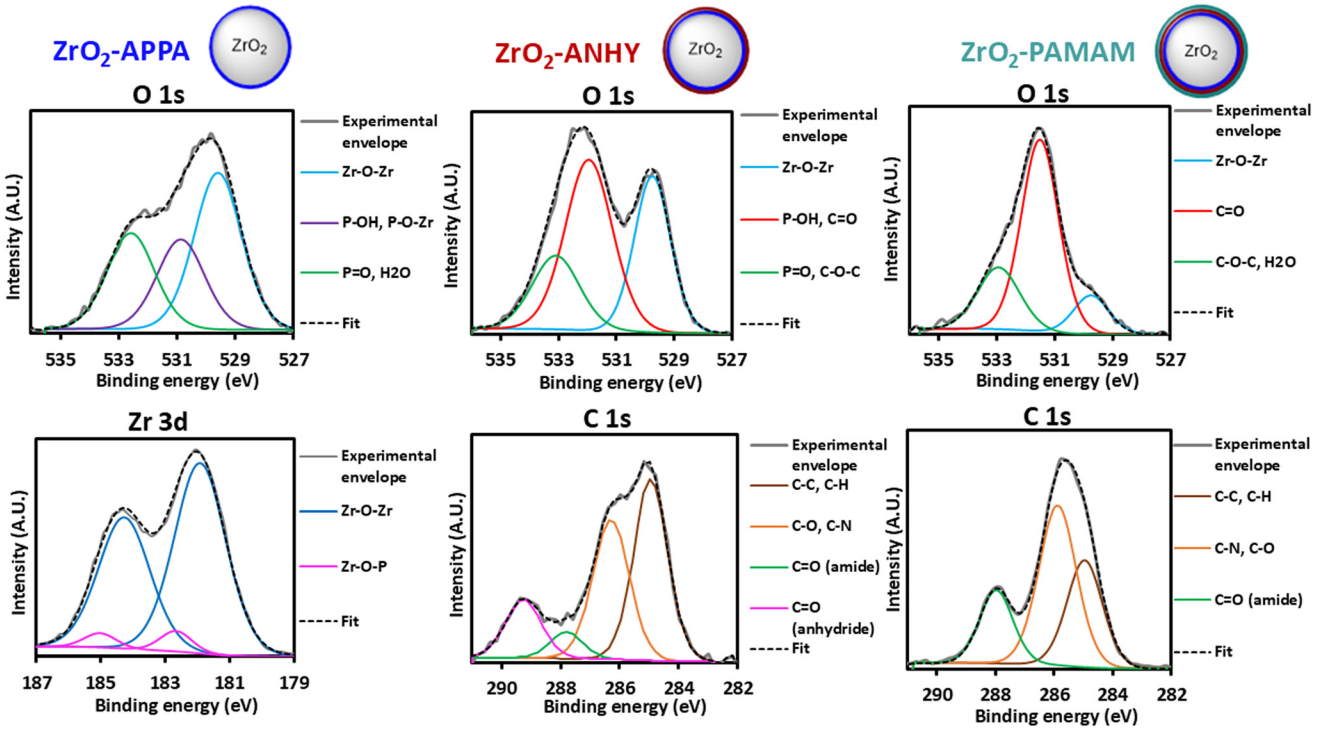

Fig. 4 XPS O 1s and Zr 3d fitting of **ZrO2-APPA** (left); XPS O 1s and C 1s fitting of **ZrO2-ANHY** (center); XPS O 1s and C 1s fitting of **ZrO2-PAMAM** (right). The deconvoluted peaks are shown in cyan blue, red, purple and green colors for O 1s; brown, orange, green and pink for C 1s; and dark blue and pink for Zr 3d. The dark dashed curve is the sum of the deconvoluted peaks and the grey curve is the experimental curve.

ively), whereas the band at 1690 cm^{-1} can be assigned to the stretching vibration of the carbonyl group of reacted species. Although the amide C═O stretching band is not clearly visible in PM-IRRAS, XPS analysis confirms the covalent bonding of ANHY by amide bonds through the appearance of the C 1s peak at 287.8 eV, characteristic of amide carbonyls.[43] Additional C 1s and O 1s signals confirm the presence of the polymer and the coexistence of anhydride and amide functions, indicating partial conversion and the availability of remaining reactive sites.

The grafting of the 4th generation PAMAM dendrimer is clearly demonstrated by PM-IRRAS, since different amide bands are observed at 1637 cm^{-1} (νC═O, amide I), 1538 cm^{-1} (δNH + νC–N, amide II) and in the 1360–1300 cm^{-1} region (amide III). The broad shoulder around 1600 cm^{-1} confirms the presence of free NH_2 groups, whereas the two bands at 1080 and 1030 cm^{-1} reveal the presence of the tertiary aliphatic amine (νN–$(CH_2)_3$) as expected for the PAMAM dendrimer. The grafting of the PAMAM dendrimer is also confirmed by XPS through the relative intensity of the C═O signal at 531.5 eV in the O 1s region (from amide functions present in the PAMAM structure), which increases significantly, while the Zr–O–Zr signal intensities decrease markedly. These observations are consistent with the presence of PAMAM on the surface. In addition, XPS experiments in the N 1s region for PAMAM-grafted samples (Fig. SII-1 in the supplementary information) showed that the chemical environment of the nitrogen atom varies from primary amine groups at the extreme surface (sputtering time = 0 s), to a predominance of amide groups at greater depths (30 s, 90 s, and 270 s). This clearly confirmed the presence of a high number of terminal primary amines from PAMAM at the outermost surface, which remain free and available for further functionalization, whereas the amide groups are located deeper within the dendrimer structure and at the interface with the polyanhydride layer. Such free NH_2-rich surfaces are ideal for the covalent anchoring of catalytic species. Hence, surface analysis using PM-IRRAS and XPS clearly demonstrated the progressive modification of the zirconia surface with the formation of covalent bonds at each step: Zr–O–P bonds with APPA, amide bonds upon coupling with ANHY, and additional amide linkages after PAMAM grafting.

Finally, a colorimetric assay, adapted from the protocol developed by Uchida *et al.*,[44] was performed to quantify the surface density of accessible primary amine groups on 1 cm diameter **ZrO_2-APPA** or **ZrO_2-PAMAM** balls. The organic dye Acid Orange 7 was used to react with available amines (see the SI for details). The mean value obtained from five replicates for the **ZrO_2-APPA** balls was 3.7 NH_2 groups per nm^2, which is consistent with the formation of a complete monolayer. This density aligns with the reported maximum calculated density of hydroxyl groups on activated zirconia surfaces (3–4 OH groups per nm^2),[45] considering that each phosphonic acid molecule reacts with one hydroxyl group. In contrast, the **ZrO_2-PAMAM** samples exhibited a significantly higher amine

density, reaching 27 NH_2 groups per nm^2, about seven times higher than that for **ZrO_2-APPA**. The quantification of the grafted catalyst (**ZrO_2-PAMAM-N** and **ZrO_2-APPA-N** samples) is not available since the colorimetric assay is dedicated to primary amines and XPS analysis cannot be performed on the balls. However, it was verified that all the primary amines present on the balls were consumed following grafting of the piperazine analogue since no colorimetric response was observed on the catalyst-grafted samples. This strongly supports the presence of piperazine moieties on the surface.

Mechanochemical conditions for the Knoevenagel condensation

With functionalized ZrO_2 balls in hand, we next focused on their use in organocatalysis for the Knoevenagel condensation, which has previously been reported in ball-milling.[31–33] Without solvent or catalyst, it was shown previously that complete conversions could be achieved for a few aldehydes using a vibratory ball-mill at 30 Hz and a planetary ball-mill at 400 rpm, highlighting the efficiency of the method.[31] Adding an organocatalyst, *i.e.* piperazine (15 mol%), afforded high yields (>80%) and was found to be compatible with a wide range of aromatic and aliphatic aldehydes.[32] We thus evaluated **ZrO_2-APPA-N** and **ZrO_2-PAMAM-N** balls in the Knoevenagel condensation of 4-chlorobenzaldehyde and malononitrile, which gave poor results without the addition of a catalyst, using a 15 mL Teflon milling jar agitated at 20 Hz in the vbm or a 20 mL ZrO_2 jar in the pbm at 250 rpm. Kinetics profiles were recorded under the same milling conditions using non-functionalized balls (Fig. 5A) and the two types of functionalized balls: **ZrO_2-APPA-N** (Fig. 5B) and **ZrO_2-PAMAM-N** (Fig. 5C) balls. Various ball sizes (0.5 and 1 cm in diameter) and numbers (1, 2, 5 and 40) were evaluated.

When using non-functionalized zirconia balls, only 17% conversion was reached after 8 h of milling (Fig. 5A). As soon as functionalized balls were used, a catalytic effect was observed, regardless of ball size, number, or functionalization type, consistently yielding full conversion into the desired product in 5–7 hours. Both ball size and number significantly increased reaction kinetics for both types of functionalized balls. The most effective conditions corresponded to the use of forty 0.5 cm diameter balls in the pbm, followed by two 1 cm-diameter balls in the vbm, then five 0.5 cm balls, and finally one 1 cm ball. The surface area of forty and five 0.5 cm balls is approximately 10-fold and 1.25-fold greater, respectively, than that of a single 1 cm ball. This total available catalytic surface area is in clear correlation with the trend in catalytic performance. Under the optimal conditions to catalyze the Knoevenagel condensation (40 **ZrO_2-PAMAM-N** balls of 0.5 cm diameter in a 20 mL zirconia jar in a pbm), complete conver-

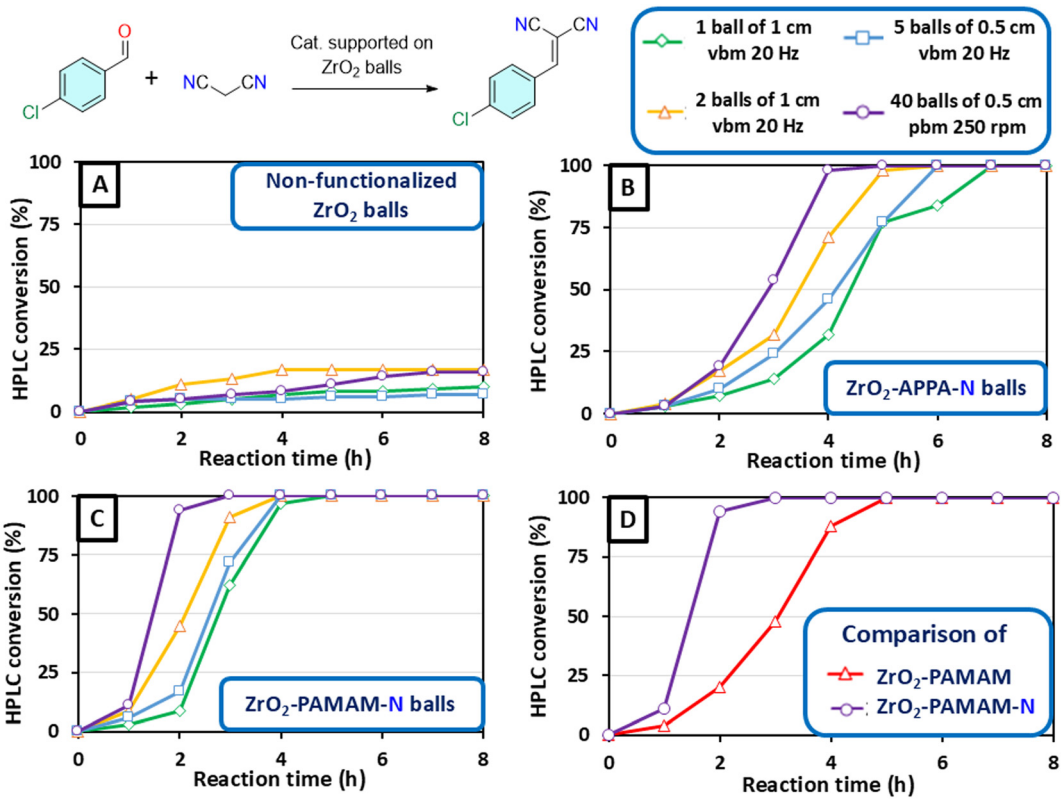

Fig. 5 Kinetics profiles of the mechanochemical Knoevenagel condensation with non-functionalized balls (A), ZrO2-APPA-N-functionalized balls (B), and ZrO2-PAMAM-N-functionalized balls (C). Graph (D) compares the kinetics profiles obtained with 40 ZrO2-PAMAM-functionalized balls and 40 ZrO2-PAMAM-N-functionalized balls, milled at 250 rpm in a planetary ball-mill.

sion was attained in 3 hours. The comparison under identical conditions with ZrO_2-**PAMAM** balls highlights the benefit of piperazine grafting, which led to improved catalytic activity (Fig. 5D). The turnover frequency (TOF), defined as the number of catalytic cycles per active site per unit of time, is calculated from eqn (1):

$$\mathrm{TOF} = \frac{n(\mathrm{product})}{n(\mathrm{active\ sites}) \times t} \quad (1)$$

where n (product) is the number of moles of product formed, n (active sites) is the number of moles of catalytically active sites on the total surface area of the ball (in this experiment 27 active sites per nm^2), and t is the reaction time. It should be noted that the reported TOF values are calculated based on the number of surface-counted active sites and therefore are not directly comparable to TOFs commonly reported for homogeneous or classical mechanochemical catalysis. Surface-normalized TOFs are nevertheless appropriate in the present case, as the catalytic activity originates from a finite number of immobilized and accessible sites on the solid support. A remarkably high TOF value of approximately 5700 h^{-1} was measured. It significantly exceeds typical values reported in the literature for Knoevenagel reactions, both in solution (typically between 50 and 400 h^{-1})[46–48] and under standard mechanochemical conditions (around 40 h^{-1}).[31,32] To assess the effect of catalyst immobilization on the milling ball, the reaction was also performed using the same amount of piperazine as that grafted onto the **ZrO_2-PAMAM-N** functionalized balls, but in its free form within the reaction medium (1.4×10^{-7} mol), which corresponds to conventional mechanochemical organocatalysis. Under these conditions, a catalytic effect was observed, but less so than with the **ZrO_2-PAMAM-N** balls as leading to complete conversion was obtained only after 4 hours (one hour longer than with the functionalized beads), resulting in a TOF of 4300 h^{-1}. This supports the theory that, in mechanochemistry, the reaction occurs primarily at the "triple contact point", where the impact involves the milling ball, the reactor wall, and all reactants including the catalyst. In our case, with the catalyst located on the ball surface, the probability of such effective collisions is increased, which is reflected in the enhanced TOF value. This result highlights the potential of such functionalized milling systems since this high TOF value strongly suggests an exceptionally active catalytic surface, highly favourable reaction dynamics under the applied mechanochemical conditions through efficient accessibility of catalytic sites, rapid diffusion under solvent-free conditions, and a synergistic effect between chemical catalysis and mechanics.

Cyclability and reaction scope

To evaluate the mechanical shock resistance of the catalytic layer grafted onto the balls, lifetime performance was assessed. Under previously optimized conditions (pbm, 250 rpm, zirconia jar, 40 **ZrO_2-PAMAM-N** balls), ten consecutive runs of the Knoevenagel condensation between 4-chlorobenzaldehyde and malononitrile were conducted. The kinetics profiles were recorded for each run by monitoring the evolution of the HPLC conversion into the desired product over time (Fig. 6).

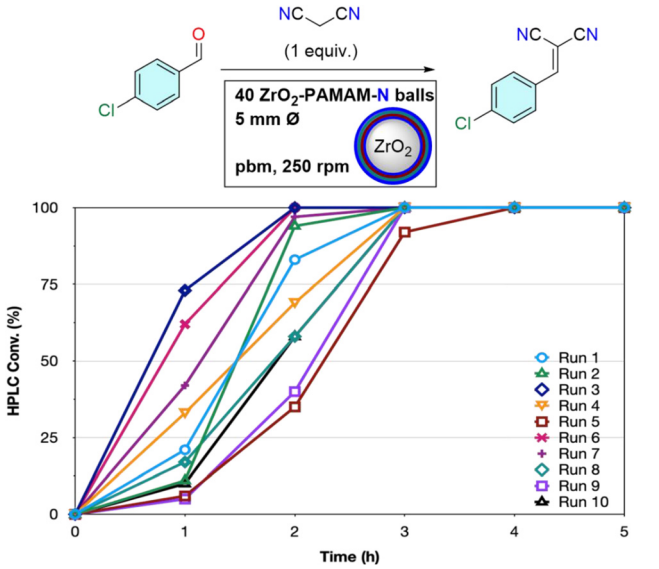

Fig. 6 Kinetics profiles obtained over ten consecutive reuse cycles of the same batch of **ZrO2-PAMAM-N**-functionalized milling balls (40 balls, 5 mm, planetary ball-mill, 250 rpm, zirconia jar of 20 mL).

For each reuse cycle, complete conversion to the desired product was achieved within 2 to 3 hours except in the fifth cycle with deviation to slightly slower kinetics. Such variations are probably related to the time required for the reagents to sufficiently agglomerate around the catalytic milling balls. This series of tests highlights the strong robustness of these organocatalyst-functionalized balls. Trace amounts of leached catalyst were evaluated by LC-MS analyses. However, no detectable catalyst-related species were observed by LC-MS, indicating that any catalyst leaching is below the detection limit of the technique. Under standard conditions and in the absence of matrix effects, the LC-MS detection limit is typically in the range of ng mL^{-1}. In the present case, assuming a worst-case scenario for catalyst leaching and considering the sampling conditions (2 mg of crude reaction mixture dissolved in 1 mL of acetonitrile), the expected catalyst concentration would be in the range of several hundred ng mL^{-1}. In consequence, the absence of any detectable signal demonstrates that catalyst leaching during the reaction, if occurring, is much less than 1% of the initial catalyst content, after 10 reuse cycles.

Finally, a systematic study of the Knoevenagel condensation reaction between various substituted aromatic aldehydes and malononitrile was conducted using **ZrO_2-PAMAM-N** milling balls in a pbm under the previously optimized conditions. Reaction performance was evaluated in terms of HPLC-determined conversion and isolated yield following simple acetone recovery and evaporation. The tested aldehydes feature a wide range of electronic substituents (electron-donating groups such as –OMe and –OH, and electron-withdrawing groups such as –Cl and $–NO_2$) and melting points spanning from –26

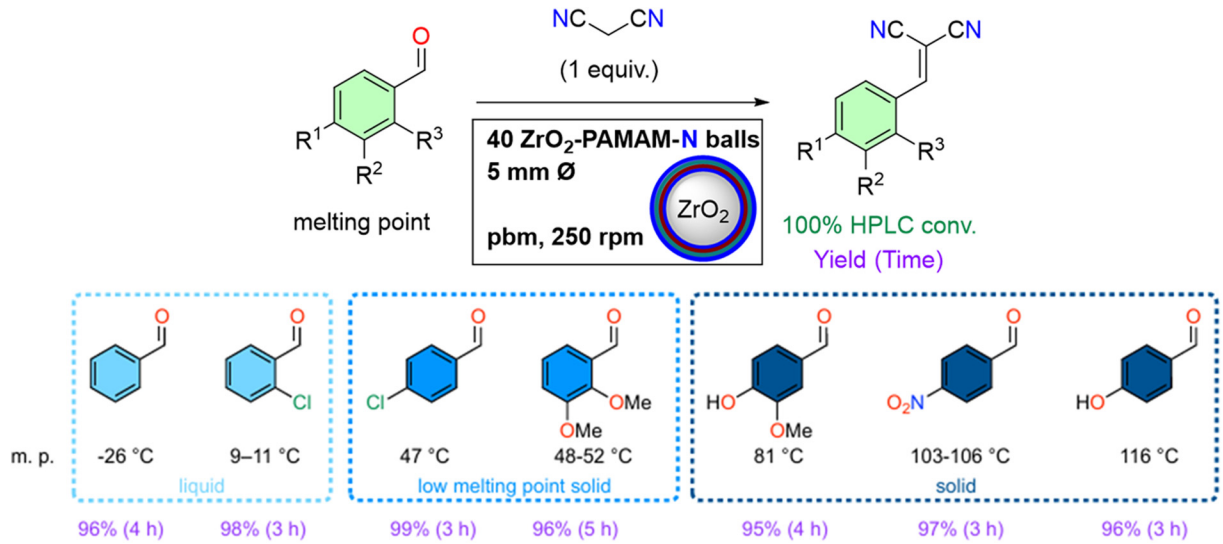

Fig. 7 Range of aromatic aldehydes with different electronic substituents and physical states, tested under direct mechano-organocatalytic Knoevenagel conditions.

to 116 °C (Fig. 7). This diversity enabled assessment of the robustness of the mechanochemical protocol, particularly with respect to aldehyde reactivity and the physical state of the reagents, which is an essential parameter in mechanochemistry as well as giving more insight into the reaction mechanisms. Of note, the same set of milling balls, recovered after washing, was used throughout the study, showing once again the reusability of the functionalized balls, even with different substrates, in the absence of contamination from the previous operation.

Remarkably, all substrates achieved 100% conversion and very high isolated yields (from 95% to 99%), highlighting the efficiency of the extraction protocol with minimal material loss. Indeed, working under stoichiometric conditions with the catalyst-supported milling balls enabled the pure Knoevenagel product to be recovered by washing the milling jar/balls with acetone, as confirmed by ^{1}H and ^{13}C NMR (see the SI). The reaction times required to reach full conversion range from 3 to 5 hours. A slightly slower kinetics was observed with two strong electron-donating groups around the aromatic ring, such as 2,3-dimethoxy or 4-hydroxy-3-methoxybenzaldehyde, but this effect remained relatively insignificant suggesting that the direct mechano-organocatalytic conditions successfully compensated for the electronically unfavorable effects. Interestingly, the physicochemical nature of the reaction medium did not appear to impact the catalytic efficiency. Whether using two liquid substrates at room temperature or a liquid/solid combination, the level of conversions into the desired products remained excellent within comparable reaction times.

Evaluation of the environmental impact

The environmental impact quantitative metrics that allow comparison of the efficiency and greenness of chemical processes were calculated.[49] Three commonly used metrics were selected: the E-factor, Reaction Mass Efficiency (RME) and Solvent Intensity (SInt). Details and formulas for these indicators are presented in supplementary information.

These metrics enable a holistic characterization of the green nature of a chemical process by integrating waste minimization, atom utilization, and solvent management considerations, thus guiding the design of more sustainable synthetic methodologies. In this study, the E-factor, RME and SI were calculated for the same chemical transformation, the synthesis of 2-amino-3-cyano-7,7-dimethyl-4-(4-chloro-phenyl)-5-oxo-5,6,7,8-tetra-4*H*-chromene. This reaction proceeds *via* a Knoevenagel condensation followed by a Michael addition. It was previously reported taking place under conventional conditions in solution[50] and in a ball-mill,[32] using 10 mol% of piperidine and 15 mol% of piperazine as catalyst, respectively, and giving the final compound in 91% yield. Using the **ZrO_2-PAMAM-N** milling balls in a pbm, full conversion was obtained after 4 h at 250 rpm, and the pure product could be recovered directly from the milling jar, without using solvent, in 95% yield.

The three green chemistry metrics were then determined for the three synthesis conditions and the results summarized in Table 1. As the amount of solvent used for purification was not specified in the literature methods (solution and classical mechanocatalytic reactions), a solvent-to-purified-product-mass ratio of 14 for the purification step was considered.

The RME is similar across the approaches (86–89%), reflecting efficient incorporation of reactants and minimal material losses during purification regardless of the method. However, direct mechano-organocatalysis drastically reduces the E-factor and, consequently, the environmental impact by eliminating solvents both during the reaction and in post-reaction purification, achieving an SI of 0. In contrast, classical mechano-

Table 1 Comparison of the environmental impact of the various strategies for the synthesis of 2-amino-3-cyano-7,7-dimethyl-4-(4-chlorophenyl)-5-oxo-5,6,7,8-tetra-4*H*-chromene

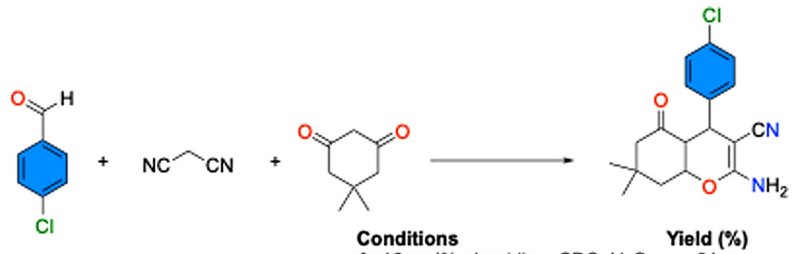

Conditions	Yield (%)
A: 10 mol% piperidine, SDS, H_2O	91
B: 15 mol% piperazine, ball-milling	91
C: ZrO_2-PAMAM-N balls, pbm	95

Piperidine or piperazine-catalyzed multicomponent reaction	E-factor	RME	SI
Conditions A (solution)[50]	22.1	86%	21.8
Conditions B (ball-milling)[32]	17.0	86%	16.8
Conditions C (direct mechano-Organocatalysis)	0.2	89%	0

chemistry only reduces the solvent used during the reaction, which is largely supplemented by the solvent used for purifications, thus limiting its overall effect as compared to solution chemistry (SI = 16.8 *versus* 21.8 in solution and E-factor = 17.0 *versus* 22.1). In comparison with conventional mechanochemical organocatalysis, where the free organocatalyst is simply added to the milling vial, catalyst immobilization enables true catalyst integration, allowing efficient separation, recyclability, and purification-free processing. The covalent anchoring of the organocatalyst prevents catalyst loss during milling, which directly accounts for the observed recyclability and contributes to the low E-factor of the process. These results demonstrate that direct mechano-organocatalysis represents a far more sustainable alternative to conventional solution-phase or classical mechanochemical methods due to it being a near solvent-free and low-waste process.

Conclusion

This work demonstrates successfully that a piperazine analogue covalently grafted onto robust, amine-functionalized zirconia balls enables direct mechano-organocatalysis in a ball-mill. Milling systems based on monolayer APPA and high-density PAMAM dendrimer grafted onto zirconia balls exhibit efficient heterogeneous catalysis. The different surface modifications were thoroughly investigated using PM-IRRAS and XPS, confirming the formation of covalent bonds at each step, and also demonstrating the sensitivity and relevance of PM-IRRAS for studying functionalized zirconia surfaces. These covalent linkages are essential not only for ensuring the chemical stability of the grafted layers but also for providing the mechanical robustness required for their application under intensive ball-milling conditions. These materials catalyzed the Knoevenagel condensation under solvent-free mechanochemical conditions with remarkable levels of performance that enable full conversion within 3 hours, high RME, a turnover frequency of 5700 h^{-1}, and a lifetime of more than 10 reuse cycles, thereby demonstrating their resistance to mechanical shock during repeated ball-milling cycles. This solvent-free and purification-free reaction generates an E-factor close to zero. These results represent the first clear demonstration of "direct mechano-organocatalysis" using organically functionalized zirconia, establishing a new paradigm for solvent-free catalysis. This green approach unlocks the untapped potential of surface-engineered ceramic materials for sustainable and reusable catalytic systems under mechanochemical conditions. Practical implementation at larger scale of this approach appear feasible as the amine functionalization of zirconia relies on simple and well-established covalent surface chemistry, and could be used for a large variety of organic catalysts. For further development of this proof-of-concept, other approaches with, for example, materials of different nature for the balls could also be interesting.

Author contributions

Conceptualization and methodology: M. G., M.-J. M., F. L., J. P., X. B. and S. D.; investigation: M. P., J. P.; data curation: all authors; writing—original draft preparation: M. P.; S. D. and M.-J. M.; writing—review and editing: all authors; supervision: M. G., M.-J. M., F. L., J. P., X. B. and S. D.; project administration resources: S. D., J. P. and X. B. All authors have read and agreed to the published version of the manuscript.

Conflicts of interest

The authors declare that they have no known competing financial interests or personal relationships that could have appeared to influence the work reported in this paper.

Data availability

The dataset supporting this study is available in the supplementary information. See DOI: https://doi.org/10.1039/d5gc06198a.

Acknowledgements

This work was funded by the French National Research Agency (ANR) under Grant FunctioMill (ANR-21-CE07-0008).

References

1 R. Šebesta, New Advances in Asymmetric Organocatalysis, *Beilstein J. Org. Chem.*, 2022, **18**(1), 240–242, DOI: 10.3762/bjoc.18.28.
2 R. Šebesta, New Advances in Asymmetric Organocatalysis II, *Beilstein J. Org. Chem.*, 2025, **21**(1), 766–769, DOI: 10.3762/bjoc.21.60.
3 D. W. C. MacMillan, The Advent and Development of Organocatalysis, *Nature*, 2008, **455**(7211), 304–308, DOI: 10.1038/nature07367.
4 S. Mukherjee, J. W. Yang, S. Hoffmann and B. List, Asymmetric Enamine Catalysis, *Chem. Rev.*, 2007, **107**(12), 5471–5569, DOI: 10.1021/cr0684016.
5 N. Marion, S. Díez-González and S. P. Nolan, N-Heterocyclic, Carbenes as Organocatalysts, *Angew. Chem., Int. Ed.*, 2007, **46**(17), 2988–3000, DOI: 10.1002/anie.200603380.
6 H. Ni, W.-L. Chan and Y. Lu, Phosphine-Catalyzed Asymmetric Organic Reactions, *Chem. Rev.*, 2018, **118**(18), 9344–9411, DOI: 10.1021/acs.chemrev.8b00261.
7 S. Dong, X. Feng and X. Liu, Chiral Guanidines and Their Derivatives in Asymmetric Synthesis, *Chem. Soc. Rev.*, 2018, **47**(23), 8525–8540, DOI: 10.1039/C7CS00792B.
8 D. Qian and J. Sun, Recent Progress in Asymmetric Ion-Pairing Catalysis with Ammonium Salts, *Chem. – Eur. J.*, 2019, **25**(15), 3740–3751, DOI: 10.1002/chem.201803752.
9 S. Shirakawa and K. Maruoka, Recent Developments in Asymmetric Phase-Transfer Reactions, *Angew. Chem., Int. Ed.*, 2013, **52**(16), 4312–4348, DOI: 10.1002/anie.201206835.
10 A. Bruckmann, A. Krebs and C. Bolm, Organocatalytic Reactions: Effects of Ball Milling, Microwave and Ultrasound Irradiation, *Green Chem.*, 2008, **10**(11), 1131–1141, DOI: 10.1039/B812536H.
11 J. G. Hernández and E. Juaristi, Recent Efforts Directed to the Development of More Sustainable Asymmetric Organocatalysis, *Chem. Commun.*, 2012, **48**(44), 5396–5409, DOI: 10.1039/C2CC30951C.
12 P. Nun, V. Pérez, M. Calmès, J. Martinez and F. Lamaty, Preparation of Chiral Amino Esters by Asymmetric Phase-Transfer Catalyzed Alkylations of Schiff Bases in a Ball Mill, *Chem. – Eur. J.*, 2012, **18**(12), 3773–3779, DOI: 10.1002/chem.201102885.
13 M. T. J. Williams, L. C. Morrill and D. L. Browne, Mechanochemical Organocatalysis: Do High Enantioselectivities Contradict What We Might Expect?, *ChemSusChem*, 2022, **15**(2), e202102157, DOI: 10.1002/cssc.202102157.
14 J. L. Howard, Q. Cao and D. L. Browne, Mechanochemistry as an Emerging Tool for Molecular Synthesis: What Can It Offer?, *Chem. Sci.*, 2018, **9**(12), 3080–3094, DOI: 10.1039/C7SC05371A.
15 J. Alić, M.-C. Schlegel, F. Emmerling and T. Stolar, Meeting the UN Sustainable Development Goals with Mechanochemistry, *Angew. Chem., Int. Ed.*, 2024, **63**(50), e202414745, DOI: 10.1002/anie.202414745.
16 K. J. Ardila-Fierro and J. G. Hernández, Sustainability Assessment of Mechanochemistry by Using the Twelve Principles of Green Chemistry, *ChemSusChem*, 2021, **14**(10), 2145–2162, DOI: 10.1002/cssc.202100478.
17 T. Friščić, C. Mottillo and H. M. Titi, Mechanochemistry for Synthesis, *Angew. Chem.*, 2020, **132**(3), 1030–1041, DOI: 10.1002/ange.201906755.
18 O. Bento, F. Luttringer, T. Mohy El Dine, N. Pétry, X. Bantreil and F. Lamaty, Sustainable Mechanosynthesis of Biologically Active Molecules, *Eur. J. Org. Chem.*, 2022, **2022**(21), e202101516, DOI: 10.1002/ejoc.202101516.
19 B. Rodríguez, A. Bruckmann and C. Bolm, A Highly Efficient Asymmetric Organocatalytic Aldol Reaction in a Ball Mill, *Chem. – Eur. J.*, 2007, **13**(17), 4710–4722, DOI: 10.1002/chem.200700188.
20 V. Némethová, D. Krištofíková, M. Mečiarová and R. Šebesta, Asymmetric Organocatalysis Under Mechanochemical Conditions, *Chem. Rec.*, 2023, **23**(7), e202200283, DOI: 10.1002/tcr.202200283.
21 D. A. Fulmer, W. C. Shearouse, S. T. Medonza and J. Mack, Solvent-Free Sonogashira Coupling Reaction Viahigh Speed Ball Milling, *Green Chem.*, 2009, **11**(11), 1821–1825, DOI: 10.1039/B915669K.
22 C. Vogt, S. Graetz, S. Lukin, I. Halasz, M. Etter, J. Evans and L. Borchardt, Direct Mechanocatalysis: Palladium as Milling Media and Catalyst in the Mechanochemical Suzuki Polymerization, *Angew. Chem., Int. Ed.*, 2019, **58**(52), 18942–18947, DOI: 10.1002/anie.201911356.
23 W. Pickhardt, C. Beaković, M. Mayer, M. Wohlgemuth, F. J. L. Kraus, M. Etter, S. Grätz and L. Borchardt, The Direct Mechanocatalytic Suzuki–Miyaura Reaction of Small Organic Molecules, *Angew. Chem., Int. Ed.*, 2022, **61**(34), e202205003, DOI: 10.1002/anie.202205003.
24 W. Pickhardt, E. Siegfried, S. Fabig, M. F. Rappen, M. Etter, M. Wohlgemuth, S. Grätz and L. Borchardt, The Sonogashira Coupling on Palladium Milling Balls—A New Reaction Pathway in Mechanochemistry, *Angew. Chem., Int. Ed.*, 2023, **62**(27), e202301490, DOI: 10.1002/anie.202301490.
25 A. J. Cummings, F. Ravalico, K. I. S. McColgan-Bannon, O. Eguaogie, P. A. Elliott, M. R. Shannon, I. A. Bermejo, A. Dwyer, A. B. Maginty, J. Mack and J. S. Vyle, Nucleoside Azide–Alkyne Cycloaddition Reactions Under Solvothermal

Conditions or Using Copper Vials in a Ball Mill, *Nucleosides, Nucleotides Nucleic Acids*, 2015, **34**(5), 361–370, DOI: 10.1080/15257770.2014.1001855.

26 C. G. Vogt, M. Oltermann, W. Pickhardt, S. Grätz and L. Borchardt, Bronze Age of Direct Mechanocatalysis: How Alloyed Milling Materials Advance Coupling in Ball Mills, *Adv. Energy Sustainability Res.*, 2021, **2**(5), 2100011, DOI: 10.1002/aesr.202100011.

27 M. Wohlgemuth, S. Schmidt, M. Mayer, W. Pickhardt, S. Graetz and L. Borchardt, Solid-State Oxidation of Alcohols in Gold-Coated Milling Vessels via Direct Mechanocatalysis, *Angew. Chem., Int. Ed.*, 2024, **63**(33), e202405342, DOI: 10.1002/anie.202405342.

28 R. A. Haley, A. R. Zellner, J. A. Krause, H. Guan and J. Mack, Nickel Catalysis in a High Speed Ball Mill: A Recyclable Mechanochemical Method for Producing Substituted Cyclooctatetraene Compounds, *ACS Sustainable Chem. Eng.*, 2016, **4**(5), 2464–2469, DOI: 10.1021/acssuschemeng.6b00363.

29 S. Shah, M. Mokhtar, T. Tran, K. Floyd, L. Mella, T. Dao, A. Garza, J. Batteas and J. Mack, Scratching beneath the Surface: Catalyst Evolution and Reusability in the Direct Mechanocatalytic Sonogashira Reaction, *RSC Mechanochem.*, 2026, **3**(1), 46–55, DOI: 10.1039/D5MR00060B.

30 A. H. Hergesell, R. J. Baarslag, C. L. Seitzinger, R. Meena, P. Schara, Ž. Tomović, G. Li, B. M. Weckhuysen and I. Vollmer, Surface-Activated Mechano-Catalysis for Ambient Conversion of Plastic Waste, *J. Am. Chem. Soc.*, 2024, **146**(38), 26139–26147, DOI: 10.1021/jacs.4c07157.

31 R. Trotzki, M. M. Hoffmann and B. Ondruschka, Studies on the Solvent-Free and Waste-Free Knoevenagel Condensation, *Green Chem.*, 2008, **10**(7), 767, DOI: 10.1039/b801661e.

32 M. Amirnejad, M. R. Naimi-Jamal, H. Tourani and H. Ghafuri, A Facile Solvent-Free One-Pot Three-Component Method for the Synthesis of 2-Amino-4H-Pyrans and Tetrahydro- 4H-Chromenes at Ambient Temperature, *Monatsh. Chem.*, 2013, **144**, 1219–1225.

33 S. Haferkamp, F. Fischer, W. Kraus and F. Emmerling, Mechanochemical Knoevenagel Condensation Investigated in Situ, *Beilstein J. Org. Chem.*, 2017, **13**(1), 2010–2014, DOI: 10.3762/bjoc.13.197.

34 P. G. Mingalyov and G. V. Lisichkin, Chemical Modification of Oxide Surfaces with Organophosphorus(v) Acids and Their Esters, *Russ. Chem. Rev.*, 2006, **75**(6), 541–557, DOI: 10.1070/rc2006v075n06abeh002478.

35 N. Gys, R. An, B. Pawlak, D. Vogelsang, K. Wyns, K. Baert, A. Vansant, F. Blockhuys, P. Adriaensens, T. Hauffman, B. Michielsen, S. Mullens and V. Meynen, Amino-Alkylphosphonate-Grafted TiO2: How the Alkyl Chain Length Impacts the Surface Properties and the Adsorption Efficiency for Pd, *ACS Omega*, 2022, **7**(49), 45409–45421, DOI: 10.1021/acsomega.2c06020.

36 D. C. Tully and J. M. J. Fréchet, Dendrimers at Surfaces and Interfaces: Chemistry and Applications, *Chem. Commun.*, 2001, **0**(14), 1229–1239, DOI: 10.1039/B104290B.

37 P. Thissen, M. Valtiner and G. Grundmeier, Stability of Phosphonic Acid Self-Assembled Monolayers on Amorphous and Single-Crystalline Aluminum Oxide Surfaces in Aqueous Solution, *Langmuir*, 2010, **26**(1), 156–164, DOI: 10.1021/la900935s.

38 A. Vega, P. Thissen and Y. J. Chabal, Environment-Controlled Tethering by Aggregation and Growth of Phosphonic Acid Monolayers on Silicon Oxide, *Langmuir*, 2012, **28**(21), 8046–8051, DOI: 10.1021/la300709n.

39 L. Sang, A. Mudalige, A. K. Sigdel, A. J. Giordano, S. R. Marder, J. J. Berry and J. E. Pemberton, PM-IRRAS Determination of Molecular Orientation of Phosphonic Acid Self-Assembled Monolayers on Indium Zinc Oxide, *Langmuir*, 2015, **31**(20), 5603–5613, DOI: 10.1021/acs.langmuir.5b00129.

40 M. G. Tammer, Sokrates: Infrared and Raman Characteristic Group Frequencies: Tables and Charts, *Colloid Polym. Sci.*, 2004, **283**(2), 235–235, DOI: 10.1007/s00396-004-1164-6.

41 X. Luo, X. Wang, S. Bao, X. Liu, W. Zhang and T. Fang, Adsorption of Phosphate in Water Using One-Step Synthesized Zirconium-Loaded Reduced Graphene Oxide, *Sci. Rep.*, 2016, **6**(1), 39108, DOI: 10.1038/srep39108.

42 S. Wu, Y. Sun, Q. Zhang, W. Si, P. Gao, L. Lu, Z. Deng, L. Xu, X. Shen and J. Liu, Elytra-Inspired Zirconium Phosphate Nanonetwork: Toward High-Quality Osseointegration and Physical-Chemical-Mechanical Bond at the Interface for Zirconia-Based Dental Materials, *Bioact. Mater.*, 2025, **50**, 116–133, DOI: 10.1016/j.bioactmat.2025.03.028.

43 Paul van der Heide, *Spectral Interpretation, X-Ray Photoelectron Spectroscopy*, John Wiley & Sons, Ltd, 2011, pp. 101–140, DOI: 10.1002/9781118162897.

44 E. Uchida, Y. Uyama and Y. Ikada, Sorption of Low-Molecular-Weight Anions into Thin Polycation Layers Grafted onto a Film, *Langmuir*, 1993, **9**(4), 1121–1124, DOI: 10.1021/la00028a040.

45 T. Joutsuka and S. Tada, Adsorption of CO2 on Amorphous and Crystalline Zirconia: A DFT and Experimental Study, *J. Phys. Chem. C*, 2023, **127**(14), 6998–7008, DOI: 10.1021/acs.jpcc.3c01185.

46 G. A. Seid, A. M. Taddesse, N. Babu and J. M. Yassin, CdS/CeO_2/Ag2CO3 Nanocomposite as an Efficient Heterogeneous Catalyst for Knoevenagel Condensation and Acetylation Reactions, *Sci. Rep.*, 2025, **15**(1), 17567, DOI: 10.1038/s41598-025-01567-1.

47 A. Chhetri, A. Maibam, S. Maniam, R. Babarao, K. Wilson, A. F. Lee and J. Mitra, A Heterogeneous Acid–Base Organocatalyst For Cascade Deacetalisation–Knoevenagel Condensations, *ChemSusChem*, 2024, **17**(24), e202400866, DOI: 10.1002/cssc.202400866.

48 P. Shekhar, V. S. Datta Devulapalli, R. Reji, H. D. Singh, A. Jose, P. Singh, A. Torris, C. P. Vinod, J. A. Tokarz,

J. J. Mahle, G. W. Peterson, E. Borguet and R. Vaidhyanathan, COF-Supported Zirconium Oxyhydroxide as a Versatile Heterogeneous Catalyst for Knoevenagel Condensation and Nerve Agent Hydrolysis, *iScience*, 2023, **26**(11), 108088, DOI: 10.1016/j.isci.2023.108088.

49 R. A. Sheldon, Metrics of Green Chemistry and Sustainability: Past, Present, and Future, *ACS Sustainable Chem. Eng.*, 2018, **6**(1), 32–48, DOI: 10.1021/acssuschemeng.7b03505.

50 G.-P. Lu and C. Cai, A Facile, One-Pot, Green Synthesis of Polysubstituted 4H-Pyrans via Piperidine-Catalyzed Three-Component Condensation in Aqueous Medium, *J. Heterocycl. Chem.*, 2011, **48**(1), 124–128, DOI: 10.1002/jhet.528.